JJEE Volume 9 | Number 4 | December 2023 | Pages 607-617

Jordan Journal of Electrical Engineering

ISSN (print): 2409-9600, ISSN (online): 2409-9619

Homepage: jjee.ttu.edu.jo

Ripple and Passive Components Reduction on All SiC Multi-Device Interleaved Boost Converter for Hybrid Electric Vehicles

Ali Zulfikaroglu[1], Amira Tandirovic Gursel[2*]

[1, 2] Department of Electrical and Electronics Engineering, Faculty of Engineering, Adana Alparslan Turkish Science and Technology University, Adana, Turkey

E-mails: agursel@atu.edu.tr; amira.t.gursel@gmail.com

Received: December 05, 2022 *Revised: April 1, 2023* *Accepted: April 10, 2023*

Abstract— Due to a smaller environmental footprint than conventional vehicles, electric vehicles (EVs) may help in the fight against climate change. In spite of their many advantages, especially those in maintenance, disadvantages such as less traveling range, long recharging time and the high price tag - compared to gas-powered vehicles - are essential barriers to extensive usage of EVs. The forenamed limitations can be partly overcome by advancing electrical equipment in terms of efficiency, weight and compactness. The development of novel materials for circuit components and improvements in circuit design have been the primary focus of advancement with regard to DC/DC converters, one of the fundamental building blocks of electrical equipment. Therefore, this paper proposes an All-SiC-based multi-device interleaved boost converter (MDIBC) to replace the Silicon insulated gate bipolar transistors (Si IGBT)-based BC topology in Toyota Prius. To achieve high efficiency from the proposed converter, the power efficiency is examined with respect to the input current ripple values. The obtained results disclose the best efficiency is achieved for a 10% input current ripple with a 50% decrease in output voltage ripple. Additionally, for these ripple values, other decisive parameters are determined and compared to the benchmark converters. The outcomes reveal that (at 70 kHz switching frequency), the best values of inductor and capacitor with reduction in their values of 83.55% and 96.45%, respectively – are achieved. This considerable decline not only results in downsizing the passive components but also leads to a higher power density that has a crucial importance for power efficiency.

Keywords— Hybrid electric vehicles; SiC MOSFET; Multi-device interleaved boost converter; Current and voltage ripples; Power efficiency.

1. INTRODUCTION

Greenhouse gases-Perfluorocarbons (PFCs), Carbon dioxide (CO2), Methane (CH4), Nitrous Oxide (N2O), Hydrofluoride carbons (HFCs), etc. are gases that can absorb infrared radiation and trap it as heat in the atmosphere. The process, also known as the greenhouse effect, is, under normal conditions, a natural and beneficial process that warms the planet trapping some portion of sunlight energy and keeping the Earth at a habitable temperature. However, the excessive release of Greenhouse gases leads to overbalanced increases in heat trapped in the atmosphere, and this extra heat causes climate change. As to reaching net-zero emissions and keeping global warming at the values specified by Kyoto Protocol, adopted in 1997, the transportation sector stands out as one of the most burning questions. In this context, in spite of many shortcomings, electric vehicles (EVs) are believed to play a vital role in realizing these aims [1, 2].

* Corresponding author

Article's DOI: 10.5455/jjee.204-1680506910

EVs can be partially or fully powered by electricity stored in drive batteries, or by two different power sources for administering driving power; and according to that, classified as Fuel Cell Electric Vehicles (FCEVs), Battery Electric Vehicles (BEVs), and Hybrid Electric Vehicles (HEVs), respectively [3]. Although EVs are becoming increasingly popular nowadays, improvements in price, capacity, driving range, losses, and power train systems are essential to compete with traditional vehicles with internal combustion engines. Accordingly, improvements in power transmission in terms of architecture and efficiency have been in the spotlight of the scientific community for decades. The power transmission system of electric vehicles consists of five main parts: battery, DC/DC converter, inverter, electric motor, and charging unit. The DC/DC converter is the power transmission circuit between the battery and the inverter block used to convert and regulate voltage from one level to another. When the vehicle is in acceleration mode, the energy in the battery is increased to the desired level before it is filtered and transferred to the inverter block. During regenerative braking, it plays a role in transferring kinetic energy to the battery. Although there are more than 500 different variants of DC/DC converters available in the continuously growing industry market [4], just a few of them is appropriate for EVs technology requiring higher output voltage levels ranging.

Boost converters (BCs) are a subgroup of DC/DC converters, appropriate for use in EVs technology where the required output voltage of the batteries ranges between 180 to 360 V to be stepped up between 400 and 750 V for the DC bus voltage [5]. BCs have many advantages, such as easy-to-drive switching components, easy-provided electromagnetic interference requirements, and low cost making them suitable for many applications in EVs technology. Additionally, efficiency can reach up to approximately 84% at full load [6, 7]. However, some drawbacks, such as high ripples of input current and output voltage and heavy and bulky passive components restricting the circuitry minimization, are major barriers to be eliminated for broader usage in EV technology.

One of the ways to cope with these problems is by designing multiphase interleaved power stages [8, 9]. A multi-device interleaved boost converter (MDIBC) is a boost converter with interleaved two phases, and each phase consists of two switches and two diodes connected in parallel. Compared to other DC/DC Converters, MDIBC has a higher efficiency. Meanwhile, it reduces not only the input current ripples that cause the battery to heat up but also the output voltage ripples that prevent the inverter from being damaged. In addition, it effectively reduces the weight and volume of the passive components, resulting in increased power density.

In this article, Toyota Prius Si IGBT-based BC is replaced by SiC-based MDIBC topology and examined for decisive parameters, before obtaining optimal ripple values for maximum effectiveness. At 40 kHz, the input current ripple values ranging from 5% to 15% were changed in 5 steps to obtain the power loss, the efficiency, and the inductor values. The highest efficiency achieved at a 10% input current ripple value was a pivot for the following examination, where the decisive parameters were examined at various frequencies. Finally, the decisive parameters were obtained for the output voltage ripple reduced to 0.25% and compared with the parameters of the benchmark converter. Calculations were performed with the 17.4 Pspice simulation software.

The rest of the paper is organized as follows: section 2 focuses on the theoretical background. For better organization of the paper, it is divided into 2 subsections. The first one deals with the characteristics of the wideband components, while the second one analyzes the decisive parameters of the circuit. In section 3, obtained simulation results and discussion are presented. The conclusions are drawn in section 4 of the paper.

2. THEORETICAL BACKGROUND

2.1. Wide Bandgap Components and Critical Parameters

Refers to switching components for MDIBC topology, where the high switching speed is strongly required due to the impact on power losses in passive components materials offering higher switching speed and manageable heat losses are naturally preferable. Until recently, the most prominent types of switches have been Silicon-based semiconductors such as Silicon Insulated Gate Bipolar Transistors (Si-IGBTs) and Silicon Metal Oxide Semiconductor Field Effect Transistors (Si-MOSFETs), frequently used in various power electronic applications. Despite several advantages, such as cost-effectiveness, high maturity, abundance in nature, and proven reliability, the theoretical performance of silicon semiconductors has been almost entirely achieved due to physical properties and characteristics.

Wide Bandgap (WBG) components such as those made of Silicon Carbide (SiC) and Gallium Nitride (GaN) have been developed to overcome the limits of Silicon-based components [10, 11]. Two good examples of those are SiC MOSFET and GaN Transistors with important features such as high band gap, large electron velocity, large critical fault electric field, and high thermal conductivity that compete against silicon IGBTs and MOSFETs. The switching frequencies of SiC-based power devices can be 10 times higher than those of Silicon-based ones. This characteristic allows for a significant reduction in the size of passive components, resulting in significantly smaller systems overall. Additionally, compared to silicon-based ones, SiC power devices can operate at significantly higher temperatures [12], hence, require less cooling, i.e. weensier heat sinks [13]. Moreover, considerably smaller power losses characteristic for all SiC components, allow utilizing smaller, more efficient batteries to get the same range while traveling farther on a single charge [14]. Hence, it can be said that SiC promises to lower system costs even if SiC-based power electronics are more expensive than conventional MOSFETs and IGBTs.

Due to the aforementioned advantages, SiC MOSFET and SiC Schottky diodes, with specifications listed in Table 1 are preferred in the study. Considering the SiC-MOSFET, Wolf speed's C3M0032120K model is preferred due to high blocking voltage with low on-resistance and high switching speed with low capacitances [15]. Thanks to these properties, it is aimed to reduce switching losses, increase the efficiency of the system and increase the power density of the system. Refers to diode components, STMicroelectronics' STPSC40H12CWL model SiC Schottky diodes are preferred due to a low V_F Schottky diode structure with a 1200 V rating preventing the appearance of reverse recovery loss during the turn-off phase as well as the decreased PCB form factor [16].

Regarding their impact on the efficiency of the circuit, there are three parameters to be examined: the conduction and switching power losses of the MOSFET and the conduction power loss of the diode. Each component is analyzed separately and losses are calculated.

Table 1. Properties of preferred SiC-based semiconductors.

Semiconductor Type			
SiC MOSFET		SiC Schottky Diode	
Manufacturer	Wolfspeed	Manufacturer	STMicroelectronics
Model	C3M0032120K	Model	STPSC40H12CWL
V_{DS}	1200 V	V_{RRM}	1200 V
I_D	63 A	$I_{F(AV)}$	2*20 A
$Rds_{(on)}$	32 mΩ	$V_{F\ (Typ)}$	1.35 V
$T_{j\ (max.)}$	175 °C	$T_{j\ (max.)}$	175 °C

The conduction power loss per each SiC MOSFET is calculated as:

$$P_{cond\_loss} = I_{ds(rms)}^2 R_{ds_{(on)}} \quad (1)$$

In Eq. (1), $R_{ds_{(on)}}$ is a drain to source ON-state resistance which is determined from the C3M0032120K datasheet, while $I_{ds(rms)}$ is the root mean square (RMS) value of the drain to source current ($I_{ds(on)}$) at the ON state represented by the following relationship:

$$I_{ds(rms)} = I_{ds(on)}\sqrt{D} \quad (2)$$

It should be pointed out that $I_{ds(on)}$ value is obtained from the current wave graph of SiC MOSFET.

The second type of power loss to be considered is the switching power loss of the SiC MOSFET, presented in Eq. (3):

$$P_{swloss} = (E_{ON} + E_{OFF})f_{sw} \quad (3)$$

E_{ON} and E_{OFF} are Turn-On and Turn-Off switching loss energies, respectively, while f_{sw} refers to the switching frequency. E_{ON} and E_{OFF} values are for corresponding I_{ds} for 650 V at a temperature of 125 °C, all of the curves used in the study are available in the C3M0032120K datasheet.

The third type of power loss taken into consideration is the conduction power loss of the SiC Schottky diode, given by the following formula:

$$P_{dcondloss} = V_F I_{(avr)} \quad (4)$$

where V_F is the forward voltage drop and $I_{(avr)}$ is the average diode current. SiC Schottky diode has no switching loss due to zero reverse recovery current. V_F value is determined using STPSC40H12CWL's datasheet, while $I_{(avr)}$ value is obtained using the current waveform of the SiC Schottky diode.

2.2. Critical Parameters Related to the Topology Itself

For a non-isolated unidirectional structure proposed instead BC topology of the benchmark converter is depicted in Fig. 1. V_{DC} is the DC power supply, V_{P1}, V_{P2}, $V_{P3,}$ and V_{P4} are pulse voltages, Q_1, Q_2, Q_3, and Q_4 are SiC-type MOSFETs, D_1, D_2, D_3, and D_4 are body diodes of MOSFETs, D_5, D_6, D_7, and D_8 are SiC Schottky diodes, L_1 and L_2 are inductors, C_o is the output capacitor, $C_{1,}$ $C_{2,}$ $C_{3,}$ C_4 are shunt capacitors, R_1, R_2, R_3, R_4 gate resistors, while R_L is the load resistor of the circuit. From the general point of view, in a MDIBC structure with the interleaved control, the switching pattern is shifted by $360°/(\boldsymbol{n}\times\boldsymbol{m})$ degrees, where m is the number of parallel connected switches per phase, while n represents the number of phases, both chosen to be 2 for proposed topology. Thanks to phase shifting, the frequency of the inductor current ripples is doubled compared to the switching frequency [17], resulting in a higher system bandwidth, which not only enhances a higher system response but also helps to minimize the size of the passive components [18]. As the shrinkage of passive components can reduce the volume and weight of the converter, it provides a valuable advantage toward a more compact structure.

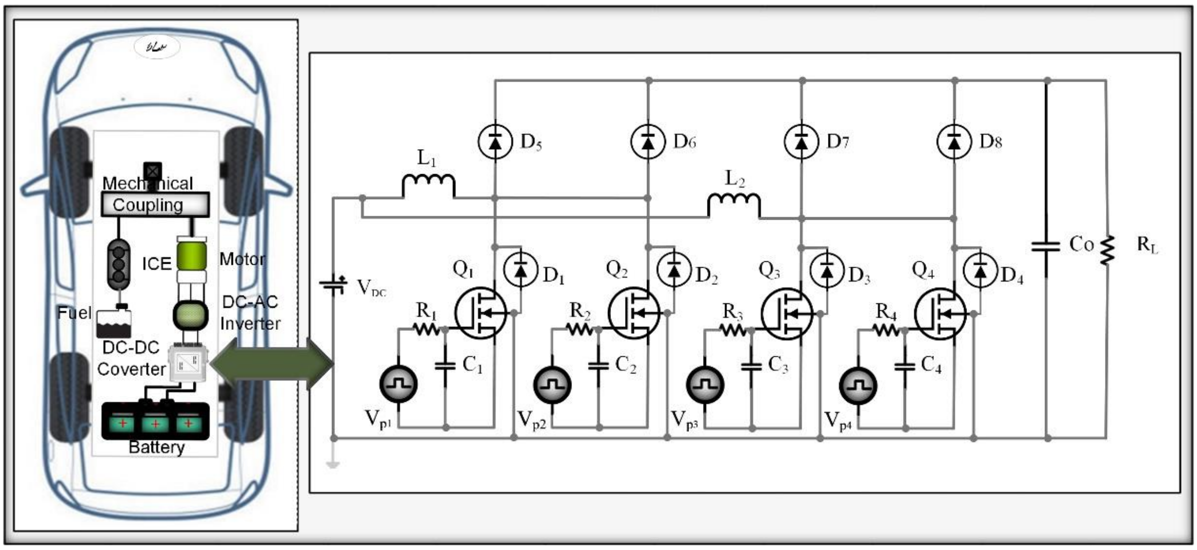

Fig. 1. The proposed non-isolated unidirectional MDIBC structure.

From the view of the impact on efficiency, three main parameters depict the circuit performance; they are the values of passive components, as the remarkable contributors to the size of the circuitry, and the converter efficiency. Assuming that the proposed converter structure is in continuous conduction mode (CCM), all the components are in the ideal characteristics, and all the switching equipment has the same duty cycle (D), the output voltage, and input current values obtained as Eqs. (5) and (6), respectively:

$$V_O = \frac{V_{in}}{1-mD} \quad (5)$$

$$I_{in} = \frac{I_{out}}{1-mD} \quad (6)$$

V_{in}, V_{out}, I_{in}, I_{out} are the input/output voltages, and input/output currents of the proposed converter, respectively. The value of mD must be less than 1.

The inductor and capacitor values can be computed by Eqs. (7) and (8), respectively. Δi and Δv values refer to input current and output voltage ripples, respectively.

$$L = \frac{V_{in}\mathrm{D}}{mnf\Delta_i} \quad (7)$$

$$C = \frac{i_{out}\mathrm{D}}{mnf\Delta_v} \quad (8)$$

Inductor loss is calculated by Inductor Designer-Micrometals Software [19] by using inductor specifications derived from [20]. A maximum operating temperature was accepted as 85 °C while the ambient temperature was estimated to be 40 °C.

The converter's efficiency can be calculated using Eq. (9).

$$\eta = \frac{P_{total}-P_{losses}}{P_{total}} \quad (9)$$

P_{total} is the total power of the converter, while P_{losses} refers to the total power loss of the converter and it is found as the sum of conduction and switching power losses of the SiC MOSFET, conduction power loss of the SiC Schottky diode and the inductor loss. It should be highlighted that the capacitor loss is neglected in this study.

3. RESULTS AND DISCUSSION

Apart from costs, the main criteria for the success of the EV converter topology are its efficiency and compactness. The only solution to increase the efficiency of any topology, and the converter is no exception, is to reduce power losses, apropos its main constituents. On the other hand, further compactness can be achieved by better placement of the electronic components and their downsizing. The main problem is a somewhat complex interconnection of their parameters. Hence, the setting should be based preferably on seeking their optimal values. That is to say, to reach the high efficiency in the proposed converter, the converter is simulated at ripple values that are predetermined so as not to exceed the passive components size of the converter to which the comparison is made.

In this direction, at the 40 kHz switching frequency, power loss, efficiency and inductor values of the topology for the current ripple of 5% and voltage ripple of 0.25% are evaluated, both considerably smaller than those in the benchmarked converter. Two critical criteria were to be considered: the ripple values should not exceed the lowest level of the benchmarked converter, and the efficiency should also stay high enough to not fall below the reference one. Dwelling on the input current ripple value is a conscience of its non-ignorable effect on inductor losses and converter efficiency as well. The converter efficiency values were tested at a switching frequency of 40 kHz for various current ripple values, to be increased from 5% to 15 %, in 2.5% steps. The results are shown in Table 2.

Table 2. SiC-based MDIBC parameters at 40 kHz with Δ_v = 0.25%.

Δi [%]	Power Loss [W]	Efficiency [%]	Inductor [μH]
5	599.32	97.780	129.95
7.5	596.45	97.790	86,94
10	594.71	97.797	64.91
12.5	600.88	97.774	51.93
15	619.79	97.704	43.4

As can be seen from Table 2, the best results for the power efficiency and the inductor value were obtained at Δ_i= 10% because a smaller inductor contributes to increased power density important for downsizing in the converter. Although the results at Δ_i= 7.5% are close to the Δ_i= 10% results, there is a clear difference between the inductor sizes at those ripple values. For this purpose, the topology was further examined at Δ_i= 10% and Δ_v = 0.25% and results are summarized afterward.

In Table 3, apart from parameters related to the proposed converters, we tabularized the parameters of the benchmarked one for a more convenient comparison. It should be highlighted that the converters can be compared only if the input voltage, output voltage, and power values are the same. The table below illustrates that current and voltage ripples decreased significantly due to multi-phase interleaved operation. Besides interleaved operation and an increased switching frequency, the passive components' value was further reduced. Moreover, comparing the two power loss data reveals that even though switching frequency increased with SiC-based MDIBC, a gain of 198.095 W was accomplished. This led to a 0.73 % improvement in efficiency.

Table 3. Parameters and simulation results of Si-IGBT-based Toyota Prius BC and SiC-Based MDIBC topology.

Parameter	Si-IGBT-Based Toyota Prius BC [21]	SiC-Based MDIBC
Input Voltage	201.6 V	201.6 V
Output Voltage	650 V	650 V
Peak Power	27 kW	27 kW
Input Current Ripple	%45.5 = 61 A	%10= 13.392 A
Output Voltage Ripple	%0.5 = 3.23 V	%0.25 = 1.625 V
Duty Cycle	0.689	0.345
Inductor Value	225.6 (μH)	2x129.83 (μH)
Capacitor Value	888 (μF)	110.21 (μF)
Switching Frequency	10 kHz	20 kHz
Total Power Loss	733.375 W	535.28
Efficiency	97.28 %	98.01 %

Using the parameters in Table 3, the proposed converter was simulated with C3M0032120K and STPSC40H12CWL semiconductors, simulation models provided by Wolfspeed [15] and STMicroelectronics [16], respectively. The proposed converter's voltage and current ripple waveforms are depicted in Figs. 2(a) and (b), respectively. As can be seen from the waveforms, the voltage and current ripples of the proposed converter meets the design requirements in Table 3. Refers to inductor-related parameters, the inductor current ripples, depicted in Fig. 2(c), are measured as 26.064 A which is about twice the input current ripple. It should be highlighted that inductors with a 180° phase difference produce an inductor current ripple that is twice as high at the same frequency.

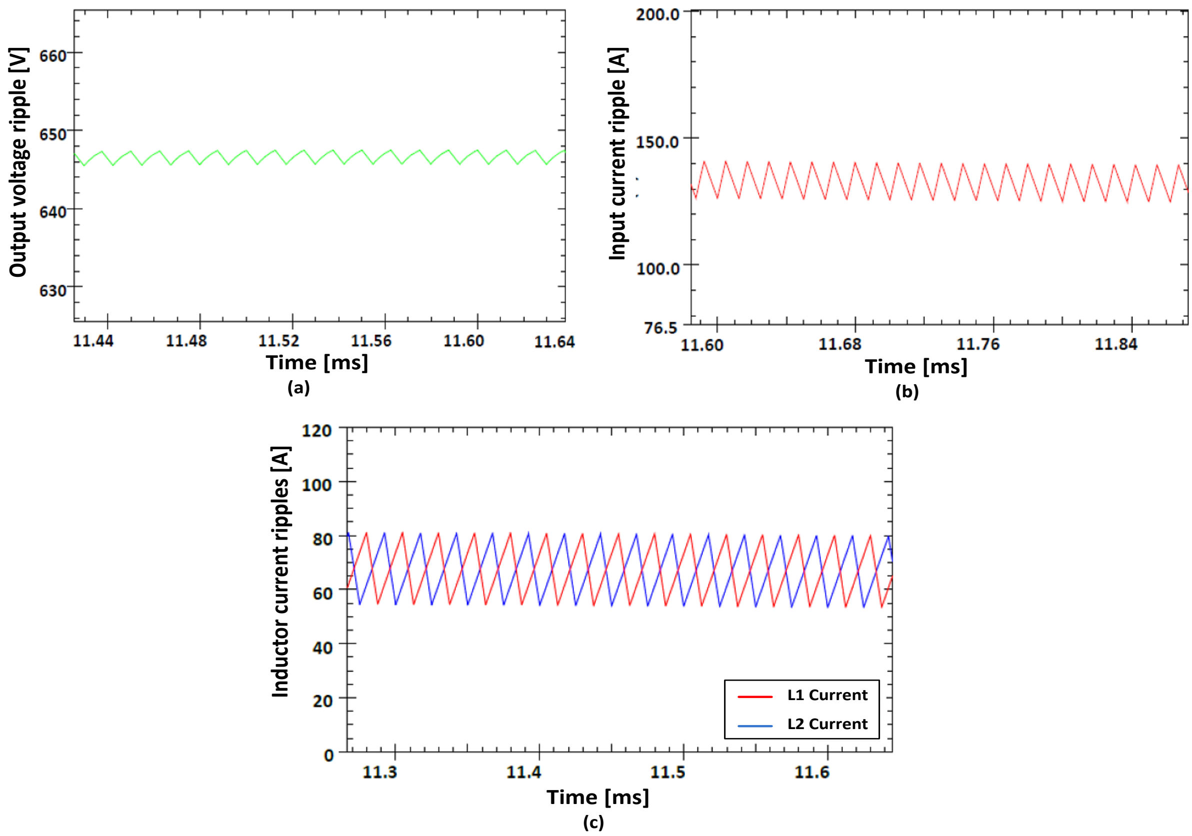

Fig. 2. Ripple waveforms of SiC-based MDIBC: a) output voltage ripple; b) input current ripple; c) the inductor current waveform of SiC-based MDIBC.

The current waveform of the SiC MOSFET, $I_{ds(on)}$, is depicted in Fig. 3(a) and used for calculations of the conduction power loss of the SiC MOSFET, which is calculated by Eqs. (1) and (2). According to the current waveform, $I_{ds(rms)}$ value is calculated as 39.177 A. The $R_{ds_{(on)}}$ value is determined as approximately 46.25 mΩ at 125 °C. With the determined values, the conduction loss of each SiC MOSFET is calculated as 70.986 W. Since there are four SiC MOSFETs in the converter, the total conduction loss of the converter is 283.95 W.

On the other hand, the switching power loss of the SiC MOSFET is calculated using Eq. (3). E_{ON} and E_{OFF} values are obtained as approximately 766.3 µJ and 322.21 µJ, respectively. Since the switching frequency is 20 kHz, the switching loss of the SiC-MOSFET is 21.77 W. Hence, the total switching power loss of the four SiC-MOSFET is found to be 87.08 W.

Regarding the conduction power losses originating from the SiC Schottky diodes, the conduction power loss per each diode is calculated using Eq. (4). The current waveform of the SiC Schottky diode (shown in Fig. 3(b)) is used in the calculation of the average diode current, $I_{(avr)}$. Due to its dual construction, the average current across the diode is doubled and obtained as 10.345 A. In the same way, the forward voltage drop is obtained as approximately 1.5 V at 125 °C. Consequently, diode conduction loss is determined to be 62.07 W in total.

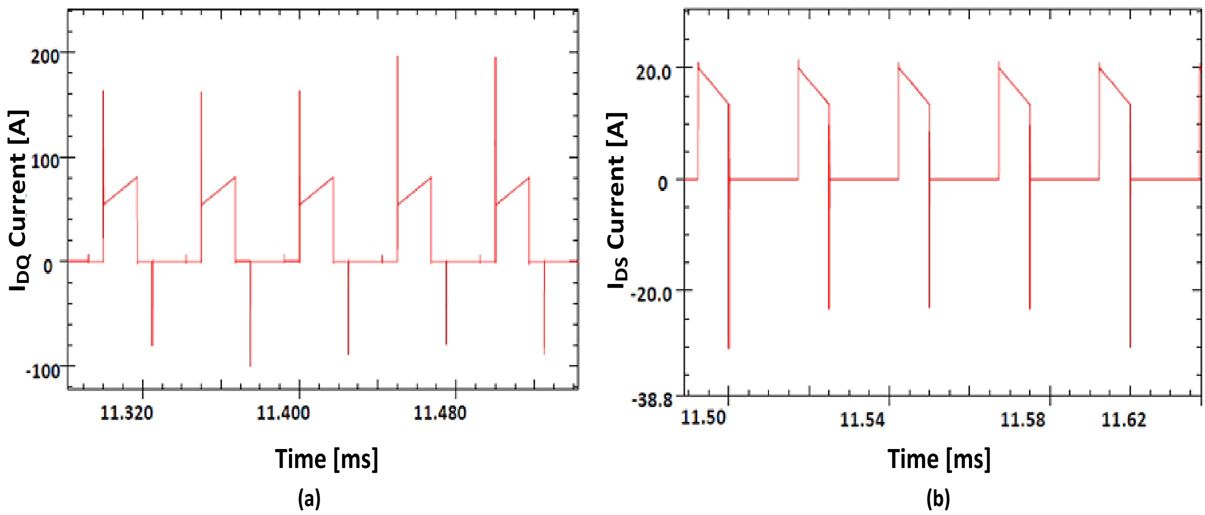

Fig. 3. Current waveform of the: a) SiC MOSFET; b) SiC Schottky diode.

With regard to passive components, the total power loss per each inductor is determined to be 51.09 W, or 102.18 W, in total. The total power loss, estimated summing up total conduction and switching losses of all components of the proposed SiC-based MDIBC, is determined to be 535.28 W. Hence, the converter's efficiency, calculated using Eq. (9), is found to be 98.01%.

Using the power loss calculation equations of the proposed converter at a switching frequency of 20 kHz, the total power losses, efficiency, and corresponding inductor and capacitor values from 20 kHz to 80 kHz at 10 kHz intervals are calculated and shown in Table 4. It is apparent from this table that the highest efficiency value was obtained at a 20 kHz switching frequency. There is a significant negative correlation between the switching frequency and passive components.

Table 4. Parameters values of the SiC-based MDIBC at different frequencies for Δ_i= 10% and Δ_v = 0.25%.

Frequency [kHz]	Total Power Loss [W]	Efficiency [%]	Inductor Value [μH]	Capacitor Value [μF]
20	535.28	98.01	129.83	110.21
30	566.33	97.90	86.56	73.47
40	594.71	97.79	64.91	55.1
50	635.38	97.64	51.93	44.08
60	678.03	97.48	43.28	36.73
70	718.87	97.33	37.09	31.48
80	760.08	97.18	32.46	27.55

The lowest inductor and capacitor values were obtained at a switching frequency of 70 kHz, still surpassing the benchmark converter in efficiency. In this frequency, the inductor value was reduced by 83.55% and the capacitor value by 96.45% according to the benchmark converter. Therefore, the size of the passive components decreased and the power density of the proposed converter increased. Lower efficiency is obtained as losses increase at 80 kHz.

Lastly, in order to provide a visual image of the results, we developed four charts, which are shown in Fig. 4. The charts provide detailed information regarding power loss, efficiency, inductor, and capacitor values at the frequencies for both scenarios. It should be noted that all charts are compared with the parameters in the benchmarked converter.

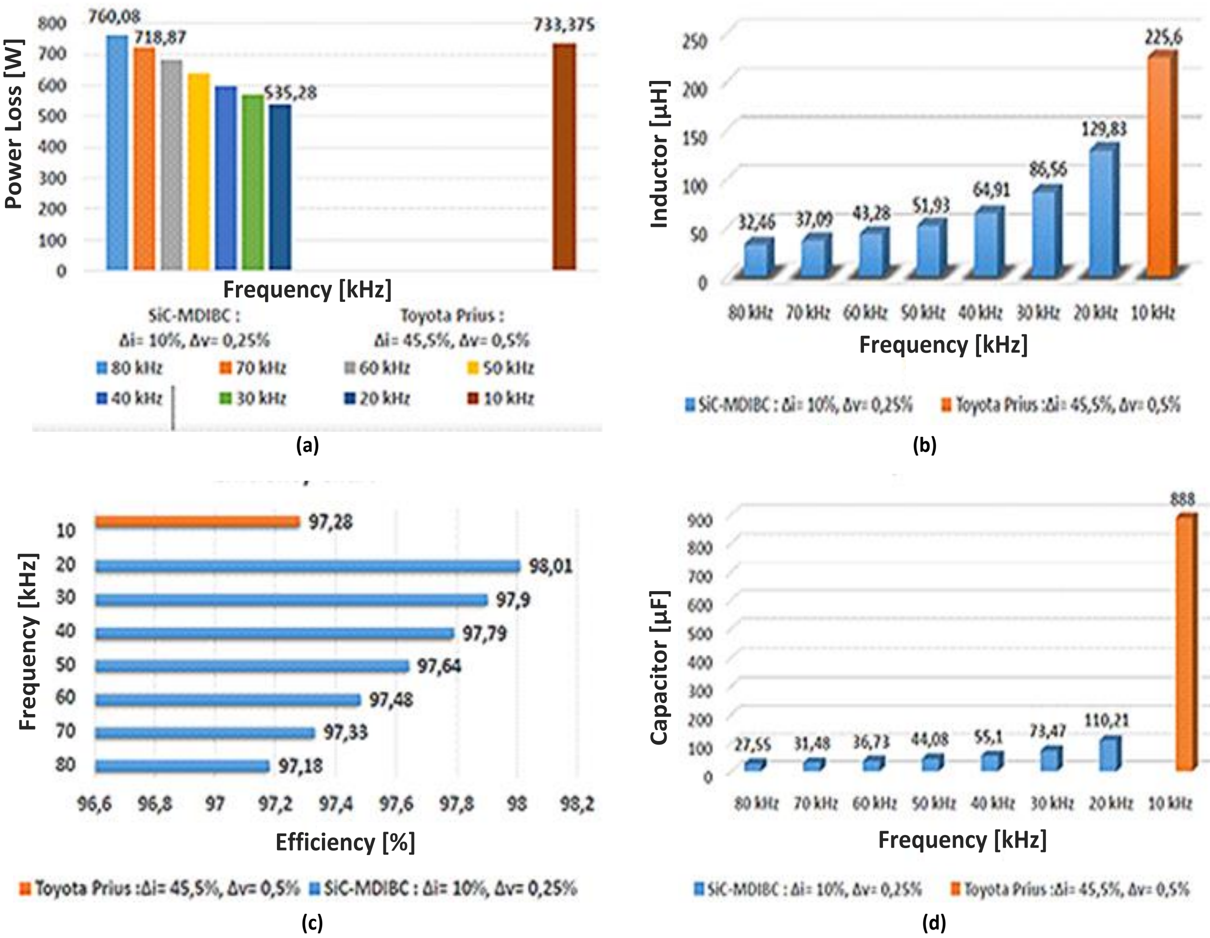

Fig. 4. a) Power loss; b) efficiency; c) inductor's size; d) capacitor size of SiC-based MDIBCs compared to Si-IGBT-based Toyota Prius.

4. CONCLUSIONS

The advantages of the MDIBC topology and the superior properties of the SiC-semiconductor can ensure valuable decreasing of voltage and current ripples, as can downsize the inductor and capacitor. These decreases are high enough to suppress both the ripples and the capacitor values of the proposed converter below the reference values. About the inductor, there is an evident juxtaposition between the determined and reference value.

This paper investigated ways for additional downsizing of the proposed SiC-based MDIBC circuit by determining the ideal ripple values that provide the highest possible efficiency. There are two critical conditions to be met when determining the best ripple values: the ripple values should not exceed those in the benchmarked converter, while the efficiency does not fall below the level of the reference converter. For this purpose, the proposed converter is simulated at a switching frequency of 40 kHz for a variety of current ripple values, from 5% to 15%, in 2.5% increments. The output voltage ripple was predetermined as 0.25%, half of the benchmark value. The optimal value of the inductor and efficiency was achieved at Δi= 10%, chosen to be starting point for further simulations. Later, the proposed converter was examined for frequencies ranging from 20 kHz to 80 kHz in steps of 10 kHz. The obtained results show that the proposed topology efficiency - as one of the decisive parameters in improving the circuitry - is higher to some degree than those in the benchmark converter, except at 80 kHz. Since additional downsizing of passive components can be obtained by increasing the switching frequency, the values of passive components are reduced up to 83.55% for the inductor, and 96.45%, for the capacitor at 70 kHz, which is a favorable impact on the weight reduction and consequently on the fuel economy. Besides, by reducing the ripple in both the input current and output voltage by 78% and 50%, we ensured that the battery and inverter generate less heat and have longer lifespans.

We believe that obtained results can be improved substantially by optimizing the decisive parameters by some of the metaheuristic optimization approaches, which will be the topic of our further study.

REFERENCES

[1] T. Lipman, M. Delucchi, "Expected greenhouse gas emission reductions by battery, fuel cell, and plug-in hybrid electric vehicles," *Electric and Hybrid Vehicles*, G. Pistoia Ed. Amsterdam: Elsevier, pp. 113-158, 2010.

[2] T. Mishra, R. Singh, "Performance analysis and hardware implementation of a dual input triple output dc-dc converter for EV application," in *2023 International Conference on Power Electronics and Energy*, pp. 1-4, 2023.

[3] O. Sen, *Performance Evaluation of Sic-Based Multidevice Interleaved Boost Converter for Electric Vehicles*, Master's Thesis, Politecnico di Milano, 2020.

[4] A. Abdelrahman, Z. Erdem, Y. Attia, M. Youssef, "Wide bandgap devices in electric vehicle converters: a performance survey," *Canadian Journal of Electrical and Computer Engineering,* vol. 41, no. 1, pp. 45-54, 2018.

[5] M. Forouzesh, Y. Siwakoti, S. Gorji, F. Blaabjerg, B. Lehman, "Step-up dc–dc converters: a comprehensive review of voltage-boosting techniques, topologies, and applications," *IEEE Transactions on Power Electronics,* vol. 32, no. 12, pp. 9143-9178, 2017.

[6] S. Chakraborty, H. Vu, M. Hasan, D. Tran, M. El Baghdadi, O. Hegazy, "DC-DC converter topologies for electric vehicles, plug-in hybrid electric vehicles and fast charging stations: state of the art and future trends," *Energies,* vol. 12, pp. 1569, 2019.

[7] M. Al Sakka, J. Van Mierlo, H. Gualous, U. Brussel, "Dc/Dc converters for electric vehicles," in *Electric Vehicles -Modelling and Simulations*, vol. 100, pp. 466, 2011.

[8] M. Azri, N. Khanipah, M. Nasir, Z. Ibrahim, A. Alias, N. Rahim, "Hardware in the loop (HIL) simulation of multi device interleaved boost converter (MDIBC)," in *2016 IEEE International Conference on Power and Energy*, pp. 155-159, 2016.

[9] R. Kumar, P. Behera, M. Pattnaik, "A comparative analysis of two-phase and three-phase interleaved bidirectional dc-dc converter," in *2023 IEEE International Students' Conference on Electrical, Electronics and Computer Science*, pp. 1-5, 2023.

[10] G. Calderon-Lopez, A. Forsyth, "High power density dc-dc converter with SiC MOSFETs for electric vehicles," in *7th IET International Conference on Power Electronics, Machines and Drives*, pp. 1-6, 2014.

[11] E. Jones, F. Wang, D. Costinett, "Review of commercial GaN power devices and GaN-based converter design challenges," *IEEE Journal of Emerging and Selected Topics in Power Electronics,* vol. 4, no. 3, pp. 707-719, 2016.

[12] W. Shi, Q. Zhang, "High performance 1200V SiC MOSFET platform with AEC-Q101 certificate," in *2022 19th China International Forum on Solid State Lighting and 2022 8th International Forum on Wide Bandgap Semiconductors*, pp. 51-54, 2023.

[13] D. Sridhar, "Silicon carbide: coming of age in electric vehicle powertrains," *E-motec,* 2022. <https://www.e-motec.net/silicon-carbide-ev-material>

[14] J. Morra, "VW opts for SiC to power future electric vehicles," *ElectronicDesign,* 2023. <https://www.electronicdesign.com/power-management/article/21259478/electronic-design-vw-opts-for-sic-to-power-future-electric-vehicles>

[15] Wolfspeed, "1200 V discrete silicon carbide MOSFETs," Products/C3M0032120K. <https://www.wolfspeed.com/1200v-silicon-carbide-mosfets/#product-table>

[16] STMicroelectronics, "1200 V, 40 A high surge silicon carbide power schottky diode," STPSCH4012C.<https://www.st.com/en/diodes-and-rectifiers/stpsc40h12c.html#cad resources>

[17] O. Hegazy, J. Mierlo, P. Lataire, "Analysis, modeling, and implementation of a multidevice interleaved dc/dc converter for fuel cell hybrid electric vehicles," *IEEE Transactions on Power Electronics,* vol. 27, no. 11, pp. 4445-4458, 2012.

[18] M. Priya, R. Balasubramanian, "Analysis of multidevice interleaved boost converter for high power applications," in *2014 International Conference on Circuits, Power and Computing Technologies*, pp. 320-327, 2014.

[19] M. Solutions, Inductor design tool. <https://www.micrometals.com/design-and-applications/design-tools/inductor-designer/>

[20] S. Öztürk, "Design of three phase interleaved dc/dc boost converter with all SiC semiconductors for electric vehicle applications," in *2017 10th International Conference on Electrical and Electronics Engineering,* pp. 355-359, 2017.

[21] T. Burress, S. Campbell, C. Coomer, C. Ayers, A. Wereszczak, J. Cunningham, L. Marlino, L. Seiber, H. Lin, "Evaluation of the 2010 Toyota Prius hybrid synergy drive system," *Oak Ridge National Laboratory Power Electronics and Electric Machinery Research Facility*, 2011.